Layer-Transfer Process for Silicon-on-Insulator with Improved Manufacturability

ALEXANDER USENKO

Silicon Wafer Technologies, Inc., Newark, NJ 07102. E-mail: usenko@si-sandwich.com

We observe hydrogen platelet buildup in single-crystalline silicon caused by hydrogen-plasma processing. The platelets are aligned along a layer of lattice defects formed in silicon before the plasma processing. The buried-defect layer is formed by either silicon-into-silicon or argon-into-silicon implantation. We discuss the platelet nucleation, growth, and merge phenomena and discuss applicability of the plasma hydrogenation to silicon-on-insulator (SOI) wafer fabrication by layer transfer.

Key words: SOI, hydrogen, silicon, implantation, platelets, plasma

INTRODUCTION

Smart-Cut is a process that allows manufacturing silicon-on-insulator (SOI) high-quality wafers in large quantities[1] that was not possible with preceding SOI processes, such as separation by implantation of oxygen. However, the Smart-Cut is still expensive because it requires hydrogen implantation in high dose, 5×10^{16} cm^{-2}.[1] Moreover, the dose should be achieved at very low ion-beam current (less then 80 μA,[2] less than 4×10^{13} ions/cm^2/s,[3] less than 0.1 mA).[4,5] Many attempts are known to reduce the dose or increase the dose rate. Most of the attempts use double-specie implantation, such as helium then hydrogen,[6–8] proving that the total dose required can be reduced to 2×10^{16} cm^{-2} in the best case. Another approach to reduce the total cost for the layer-transfer process has been suggested in Refs. 9–15, where hydrogen is delivered by diffusion to a buried trap layer in silicon. Here, we are continuing that approach while using plasma for the hydrogenation.

The International Technology Roadmap for Semiconductors 2001[16] projects that the cap-Si layer for SOI starting wafers will be 20–100 nm in thickness by 2004 to support processing of fully depleted, complementary metal-oxide semiconductor circuits. Smart-Cut provides an inherent-Si film thickness of about 500 nm and a minimum thickness of about 200 nm.[17] The thickness of the delaminated layer in the Smart-Cut process depends on the energy of the implantation of hydrogen. When the energy of the H implant is reduced below 20 keV to achieve thin delaminating thickness, problems arise.[7] Attempts have been reported to obtain a thin (<200 nm) cap-Si layer of SOI wafers. Qian et al.[7] and Qian and Terreault[18,19] used low-energy hydrogen implantation (5–8 keV) in a regular Smart-Cut to get a thinner top SOI layer. They concluded keV-range hydrogen implant does not set up layer transfer. Maleville et al.[20] reports 70-nm, top-Si SOI using touch polishing of an initial 500-nm layer. Srikrishnan[21] forms (by implantation) an etch-stop layer inside of the film transferred with Smart-Cut with a subsequent etching. Popov et al.[22] reports a layer-by-layer oxidation (of the film transferred with Smart-Cut) with subsequent stripping in diluted HF for thinning of the layer. All listed approaches increase SOI wafer-production cost and degrade thickness uniformity. Our work here reports plasma hydrogenation as a post process, following a low-level implant to create the desired cap layer of thickness less than 100 nm.

(Received October 1, 2002; accepted March 10, 2003)

EXPERIMENTAL

Variously doped Si ⟨100⟩ wafers were implanted with Si at 180 keV, 2×10^{15} cm^{-2}. Some samples were implanted with argon at 180 keV, 1×10^{15} cm^{-2}. Then, the as-implanted samples were processed with radio-frequency (RF) hydrogen plasma for ~1 h at 300-W RF power, and 1-mtorr hydrogen pressure. The samples were kept at 200°C during the first 30 min, and then, the sample temperature was increased to 300°C. Some wafers were annealed at 550°C to initiate blistering. The wafer surfaces were analyzed with an atomic-force microscope.

Table I. Experimental Conditions

Wafer		
Diameter		100 mm
Growth		Czochralski
Dopant		Boron
Resistivity		1 Ω cm
Implantation		
Species	$Silicon^{+}$	$Argon^{++}$
Energy	180 keV	395 keV
Dose	2×10^{15} cm^{-2}	1×10^{15} cm^{-2}
Hydrogenation		
Source		RF plasma
Plasma power		300 W
Temperature, 1st step		200°C
Duration, 1st step		30 min
Temperature, 2nd step		350°C
Duration, 2nd step		1 h

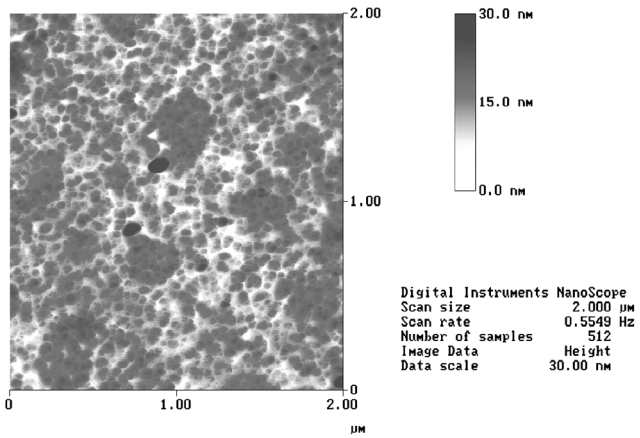

Fig. 1. A surface relief developed on a self-implanted silicon wafer after plasma hydrogenation, (area of view 2 × 2 μm^2).

Infrared-absorption measurements were performed using both transmission and multiple internal-reflection geometries[23] to gain access to both bending and stretching vibrations of trapped hydrogen. The processing conditions are summarized in Table I. Layer-transfer experiments were also performed. Prebonding, cleavage, and post-bonding steps were performed as in the Smart-Cut process. The thickness of the transferred layers was measured with a Dektak profilometer near the wafer edges where the layer transfer fails.

RESULTS

Figures 1 and 2 show the surface of a wafer processed by self-implantation + hydrogenation and annealed at 550°C. The surface is covered with features of lateral dimensions of about 0.2 μm and vertical dimension about 5 nm. Infrared measurements of unannealed samples (Fig. 3) show strong hydrogen peaks. Additional layer-transfer experiments show successful layer transfer (Fig. 4) even for much shorter plasma-processing time than needed to develop the surface relief shown in Figs. 1 and 2.

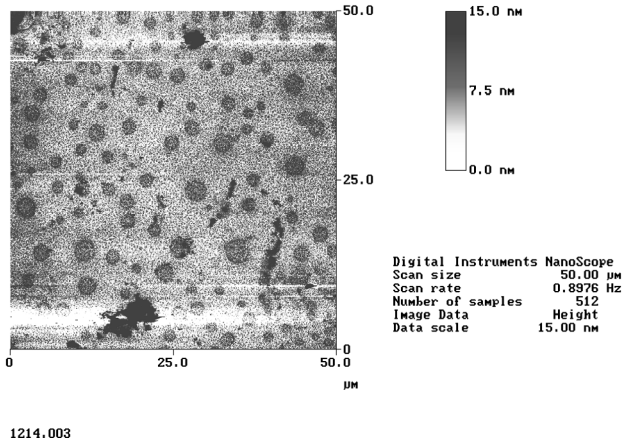

Fig. 2. A surface relief developed on a self-implanted silicon wafer after plasma hydrogenation, (area of view 50 × 50 μm^2).

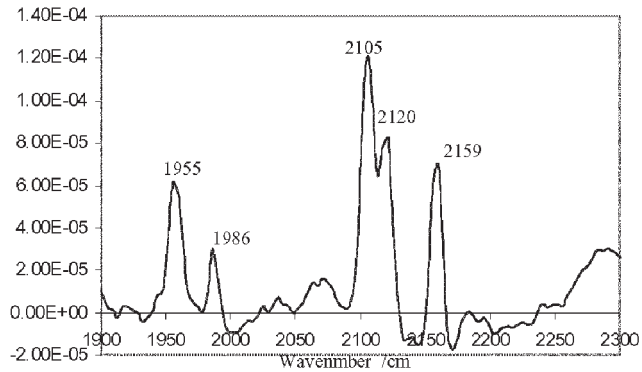

Fig. 3. The profile near the edge of the transferred layer.

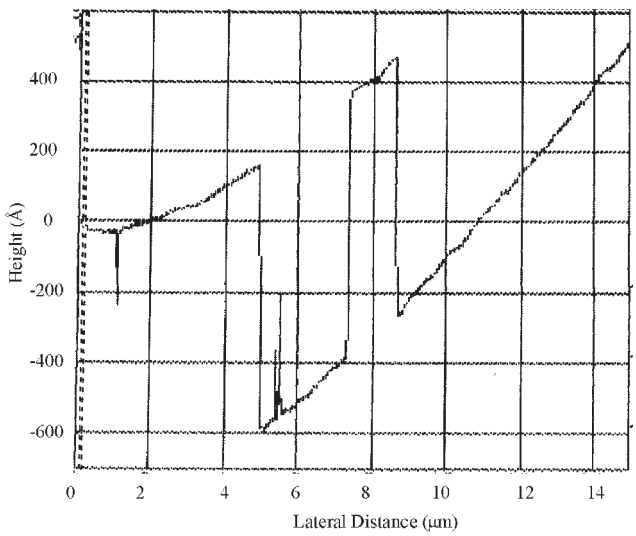

Fig. 4. The infrared spectra of the hydrogenated sample. The 1955 and 1986 peaks relate to Si-H, and 2105, 2120, and 2159 peaks relate to molecular hydrogen attached to internal surfaces in Si.

The layer transfer occurs in cases of proper selection of implantation conditions and plasma-hydrogenation conditions. A typical edge profile of the transferred layer is shown on Fig. 4. The thickness of the transferred layer is 75 nm. Similar results are

obtained for some other heavier ions that penetrate less deeply.

Infrared-absorption measurements (Fig. 3), taken on samples processed at 300°C during the second plasma-immersion step, indicate that hydrogen is primarily located on internal surfaces with some H still in monovacancy-type defects, such as VH and VH_3, consistent with previous studies.[23] Further studies are under way to characterize the nature and location of hydrogen incorporated in the silicon as a function of processing conditions.

DISCUSSION

Hydrogen in atomic form is known for its high diffusivity in silicon and its ability to combine with many types of defects in crystalline silicon. It has been known since 1987 that plasma hydrogenation of regular single-crystalline silicon results in the formation of hydrogen platelets.[24,25] Because of a lack of defects in bulk silicon and low hydrogen solubility in silicon, the platelets in these earlier works are found near the surface in defect-rich regions only. To control the process of hydrogen-platelet distribution in silicon, an additional step of forming a defect-rich layer is needed. To accumulate the hydrogen in the desired part of the wafer, we need to preform defects that readily interact with hydrogen. Silicon-into-silicon implantation allows forming a dense defect layer at the desired depth under the surface. Low-soluble gas (He, Ar, Ne, Kr, or Xe) implantation is another option to form the trap layer. Use of heavier implants, such as xenon, allows the reaching of extremely thin transferred layers, approximately tens of nanometers. Figure 7 shows Stopping and Range of Ions in Matter (SRIM) simulations for R_p for hydrogen and xenon, and the R_p for 50-keV xenon is about 30 nm.

The RF plasma causes a platelet nucleation and growth along a layer at a depth of about R_d (depth of the maximum of the vacancy-type defects) of the defect-inducing implant. The lower temperature-plasma process is for nucleation, and the 300°C step is for fast platelet growth, similar to Refs. 24 and 25. A significant difference we found comparing hydrogenation results for self-implanted and argon-implanted samples is that for the self-implanted samples the first low-temperature step is required to get blistering, while for the argon-implanted samples the low-temperature step can be skipped. A possible explanation is that the argon-implanted samples already contain the platelet nuclei in form of argon microbubbles, while in the self-implanted samples, the platelet nuclei should be first formed from vacancy clusters. As compared to the surface features observed on heavily hydrogen-implanted wafers in the literature,[1,7,8,18,23] the features in Figs. 1 and 2 have about 10 times smaller lateral and 100 times smaller vertical dimensions.

An inherent delaminating thickness for either the Smart-Cut or the trap-filling process is controlled by implantation depths.[1,7,8] For Smart-Cut, the depth is the R_d of the hydrogen implant, while for the trap-filling process, the R_d of the heavier ions is used. Correspondingly, 200–2,000-nm and 20–200-nm layers are transferred, respectively, for each process. Therefore, the trap-filling process is advantageous for making thin SOI.

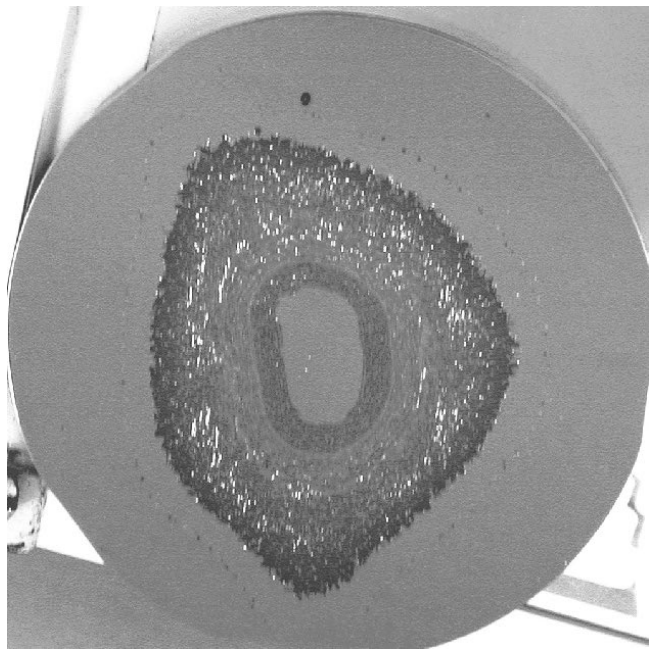

Fig. 5. A typical wafer blistered during implantation. Implantation conditions: H_2^+ at 100 keV, 0.3 mA.

Experiments with blistering were widely used elsewhere to understand phenomena involved in the Smart-Cut process.[3,9,14] At the level of hydrogen implantation required in Smart-Cut (i.e., about 5×10^{16} cm^{-2}), the silicon surface easily blisters during implantation (Fig. 5), even without an additional annealing. The silicon-wafer surface can be also blistered after RF-plasma hydrogenation. An interesting feature is that the minimum hydrogenation time in RF plasma required for blistering is several times longer than the time required for successful layer transfer. Typical blistering pictures after RF-plasma hydrogenation and subsequent anneal are shown in Figs. 1 and 2. We suppose that in blistering experiments, hydrogen loss is much higher because of out-diffusion compared to the case of layer transfer. These hydrogen losses may be due to the proximity of the surface or due to a difference in the type of the traps binding the hydrogen. When the hydrogen-rich layer (either obtained by trapping or by implantation) evolves into a quasi-continuous cleavage plane, the hydrogen atoms or molecules detach from one defect, diffuse to another defect with higher bonding energy, and get trapped again. In a case of high-dose hydrogen implantation, a higher mechanical stress is expected leading to weakened silicon bonds and higher bonding energy for hydrogen attaching to those sites.

In Smart-Cut, to keep a large amount of hydrogen inside the silicon wafer, the local temperature under

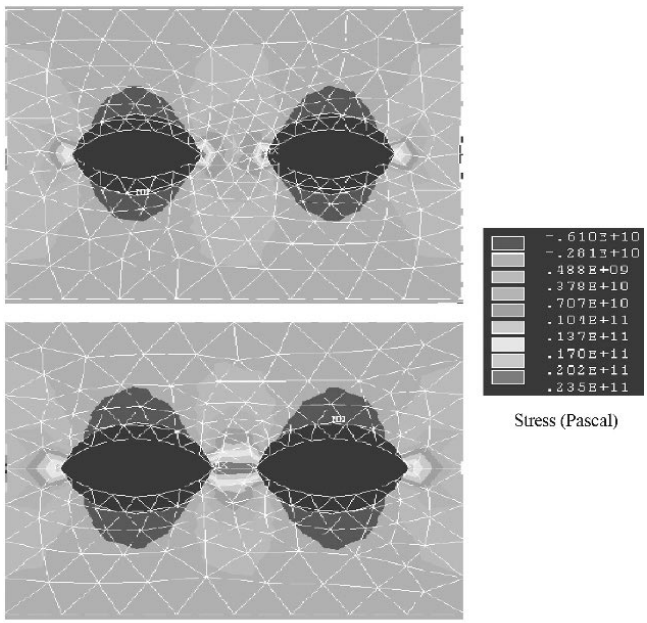

Fig. 6. A computer simulation of evolution of two neighboring microbubbles with increasing pressure inside of the bubbles. The bubbles are the black ovals. The top picture has a lower pressure compared to the bottom picture. Note that the tensile stress substantially increases (indicated by red regions) between the bubbles with increasing pressure.

the beam should not substantially exceed room temperature. This restriction severely limits the maximum, hydrogen ion-beam current during the implantation step. As reported by several researchers including us,[2–5] the hydrogen-beam current should be kept below 0.1 mA to prevent blistering of the wafers using conventional implanters. However, at this beam current, hydrogen implantation for Smart-Cut will take 24 h to fully implant 300-mm wafers.

At the beginning of plasma hydrogenation, atomic hydrogen diffuses through silicon and attaches to broken bonds in a layer damaged by implantation.[11] The next step in hydrogen evolution is to form nuclei of hydrogen platelets. This happens at temperatures lower than 250°C, as previously found by Nickel et al.[24] and Johnson et al.[25] Further hydrogenation increases the platelet size and can be done at higher temperatures. Higher temperature during the second stage of hydrogenation is also needed to allow Oswald ripening during which time larger platelets grow at the expense of smaller ones.[24,25] By collecting the hydrogen from the hydrogen-rich layer, the platelets transform into microbubbles.[23] The neighboring microbubbles continue to coalesce, as predicted by computer simulation (Fig. 6).

As we have shown previously, the hydrogen-dose rate severely limits Smart-Cut. Higher implant rates might be acceptable using implanters with a special cooling system, but there are no published data yet that confirms efficiency of the cooling for the Smart-Cut process. Also, the cooled-wafer surface effectively adsorbs residual gases from the implantation chamber and that adsorbed species immediately undergoes ion mixing by continuing hydrogen implantation. This results in heavy contamination in the cap layer of the SOI substrate. In our process, neither high-dose implantation nor hydrogen implantation are needed, thus making our process potentially advantageous. Also, the typical implantation doses needed to form the trap layer is lower than 10^{15} cm^{-2}, which might result in better crystalline quality of the cap layer in the final SOI wafer as compared to the Smart-Cut process.

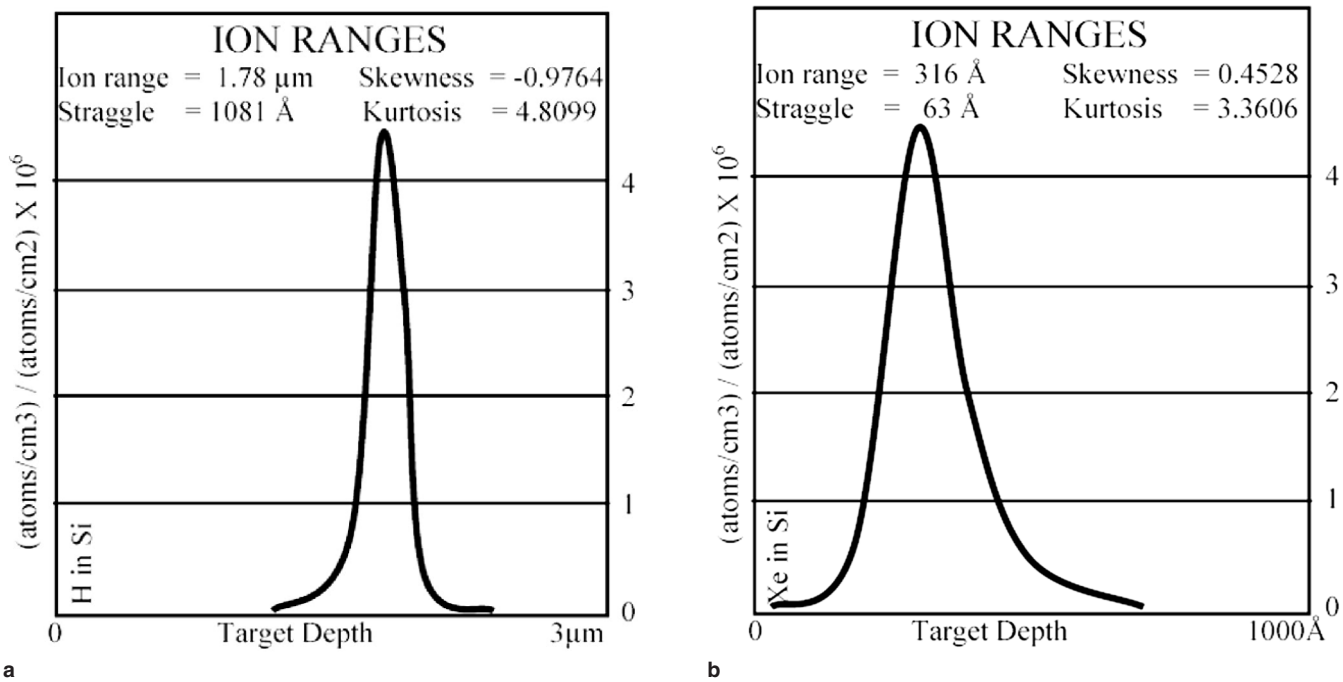

Fig. 7. The SRIM simulation of projected ranges for (a) H^+ 200 keV and (b) Xe^+, 50 KeV giving 1,660 nm and 31 nm, respectively.

CONCLUSIONS

The RF-plasma hydrogenation of a buried trap layer formed with low-dose ion implantation has been demonstrated for forming SOI with a thin cap layer. Experiments described here indicate that the trap-filling process can provide a 10 times reduction in SOI cap-layer thickness.

ACKNOWLEDGEMENTS

Partial funding from National Science Foundation SBIR Award No. DMI-0216676 is gratefully acknowledged.

REFERENCES

1. B. Aspar et al., *J. Electron. Mater.* 30, 834 (2001).
2. K. Henttinen, I. Suni, and S.S. Lau, *Appl. Phys. Lett.* 76, 2370 (2000).
3. Y. Zheng, S.S. Lau, T. Höchbauer, A. Misra, R. Verda, X.-M. He, M. Nastasi, and J.W. Mayer, *J. Appl. Phys.* 89, 2972 (2001).
4. T. Suni, A. Nurmela, I. Suni, S.S. Lau, T. Hochbauer, M. Nastasi, V.-M. Airaksinen, and K. Henttinen, *Nucl. Instrum. Meth. B* 190, 761 (2002).
5. W.N. Carr, B. Chen, A.Y. Usenko, and Y. Chabal, *2002 IEEE/SEMI Advanced Semiconductor Manufacturing Conf. Proc.* (Piscataway, NJ: IEEE, 2002), pp. 6–10.
6. A. Agarwal, T.E. Haynes, V.C. Venezia, O.W. Holland, and D.J. Eaglesham, *Appl. Phys. Lett.* 72, 1086 (1998).
7. C. Qian, B. Terreault, and S.C. Gujrathi, *Nucl. Instrum. Meth. B* 175–177, 711 (2001).
8. Q.-Y. Tong, R. Scholz, U. Gösele, T.-H. Lee, L.-J. Huang, Y.-L. Chao, and T.Y. Tan, *Appl. Phys. Lett.* 72, 49 (1998).
9. A.Y. Usenko and W.N. Carr, in: *Silicon-on-Insulator Technology and Devices X,* ed. S. Cristoloveanu (Pennington, NJ: The Electrochemical Society, 2001), pp. 33–38.
10. A.Y. Usenko and W.N. Carr, *Mater. Res. Soc. Symp. Proc.* 681E, I3.3.1 (2001).
11. A.Y. Usenko and W.N. Carr, *Proc. 2000 IEEE SOI Conf.* (Piscataway, NJ: IEEE, 2000), pp. 16–17.
12. A.Y. Usenko, U.S. patent 6,368,938 (9 April 2002).
13. A.Y. Usenko, U.S. patent 6,352,909 (5 March 2002).
14. A.Y. Usenko and W.N. Carr, U.S. patent 6,346,459 (12 February 2002).
15. A.Y. Usenko, U.S. patent 6,344,417 (5 February 2002).
16. European Electronic Component Manufacturers Association and International SEMATECH, *The International Technology Roadmap for Semiconductor* (San Jose, CA: Semiconductor Industry Association, 2001), p. 7.
17. General specification for customized UNIBOND® Wafers, SOITEC, Parc technologique des Fontaines, 38190 Bernin, France, 2002.
18. C. Qian and B. Terreault, *J. Appl. Phys.* 90, 5152 (2001).
19. C. Qian and B. Terreault, *Mater. Res. Soc. Symp. Proc.* 585, 177 (2000).
20. C. Maleville, E. Neyret, E. Ecarnot, L. Arene, T. Barge, and A.J. Auberton, *2001 IEEE Int. SOI Conf.* (Piscataway, NJ: IEEE, 2000), pp. 155–156.
21. K.V. Srikrishnan, U.S. patent 5,882,987 (16 March 1999).
22. V.P. Popov, I.V. Antonova, V.F. Stas, L.V. Mironova, A.K. Gutakovskii, E.V. Spesivtsev, A.S. Mardegzhov, A.A. Franznusov, and G.N. Feofanov, *Mater. Sci. Eng. B-Solid* B73, 82 (2000).
23. M.K. Weldon et al., *J. Vac. Sci. Technol. B* 15, 1065 (1997).
24. N.H. Nickel, G.B. Anderson, N.M. Johnson, and J. Walker, *Phys. Rev. B* 62, 8012 (2000).
25. N.M. Johnson, F.A. Ponce, R.A. Street, and R.J. Nemanich, *Phys. Rev. B* 35, 4166 (1987).